DALTON
FULL PAPER

Low temperature stopped-flow studies in inorganic chemistry †

Markus Weitzer,[a] Markus Schatz,[a] Frank Hampel,[b] Frank W. Heinemann[a] and Siegfried Schindler *[a]

[a] *Institute of Inorganic Chemistry, University of Erlangen-Nürnberg, Egerlandstrasse 1, 91058 Erlangen, Germany. E-mail: schindler@chemie.uni-erlangen.de*
[b] *Institute of Organic Chemistry, University of Erlangen-Nürnberg, Henkestrasse 42, 91054 Erlangen, Germany*

Received 3rd September 2001, Accepted 14th November 2001
First published as an Advance Article on the web 25th January 2002

Low temperature stopped-flow methods together with diode array instrumentation have become extremely useful for studying reactions that are too fast at ambient temperatures and/or for detecting reactive intermediates that can only be observed at low temperatures. Furthermore, global analysis fitting methods are described that allow the analysis of complex reaction mechanisms. To illustrate the method the reaction of dioxygen with the tripodal copper(I) complex [Cu(Me$_2$-uns-penp)(CH$_3$CN)]ClO$_4$ (Me$_2$-uns-penp = (2-dimethylaminoethyl)bis(2-pyridylmethyl)amine) is discussed as an example.

Introduction

In the last decade, mainly as a consequence of the advances in computer technology, instrumentation for kinetic investigations has improved dramatically. For example a stopped-flow unit in the late eighties consisted of a large number of different parts, which included: the syringe system, a lamp together with a monochromator, an oscilloscope for viewing the data and a transient recorder for collecting the data and for their transfer to a computer for data fitting. Many problems occurred during these measurements and they were time consuming because programs for analysing the data were still slow once absorbance *vs.* time traces were observed that could not be fitted to a single exponential function. Furthermore, only measurements at single wavelengths were possible, therefore making it often necessary to repeat the analysis at different wavelengths.

Today a stopped-flow instrument consists of only the unit itself combined with a diode array setup and a computer allowing fast kinetic measurements of time resolved UV-vis spectra under anaerobic conditions, high pressure and/or low temperatures. Improvements have been made here as well: *e.g.* syringes are installed vertically instead of horizontally (to avoid problems with gas bubbles) and peek (polyetheretherketone) is used instead of Teflon for valves and flow tubes to improve the anaerobic capabilities of the instrument. Furthermore, the syringe drives setup was optimized. Companies offering modern stopped-flow equipment are Hi-Tech Scientific (Salisbury, UK), Applied Photophysics Ltd. (Leatherhead, UK), Bio-Logic-Science Instruments SA (Claix, France), Olis Incorporated (Bogart, GA, USA) and KinTek Corporation (Austin, TX, USA).

We employ extensively the stopped-flow technique for the investigation of the reaction of dioxygen with copper(I) complexes.[1–9] Such compounds can be regarded as low molecular weight model complexes for a large number of copper proteins involved in the redox processing of dioxygen.[7,10–19] They not only provide a better understanding of the biological molecules but also assist in the development of new homogeneous catalysts for selective oxidations under mild conditions.[20]

A whole variety of copper dioxygen adducts can form when copper(I) complexes react with dioxygen.[7,19] The course of these reactions depends on the temperature, ligand and solvent.[7,19] Therefore, it is of great interest to elucidate the reaction mechanisms of the binding and activation of dioxygen by copper(I) complexes.

The first example of a structurally characterized copper peroxo complex was obtained by Karlin and co-workers from the reaction of [Cu(tmpa)(CH$_3$CN)]PF$_6$ (tmpa = tris[(2-pyridyl)-methyl]amine, Scheme 1) with O$_2$ at low temperatures.[21,22]

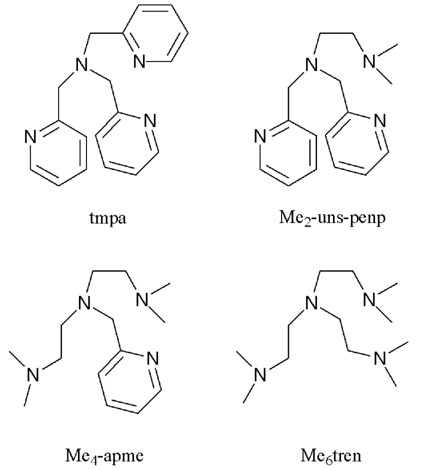

Scheme 1

A detailed kinetic investigation of the reversible reaction of [Cu(tmpa)(CH$_3$CN)]$^+$ with O$_2$ was performed at low temperatures in propionitrile, which allowed the spectroscopic observation of a superoxo complex prior to the formation of the peroxo complex.[23] Furthermore, the influence of steric hindrance as well as different donor atoms in the ligand on the formation of the peroxo complexes was studied.[23,24] Recently, we have investigated the effect of the chelate ring size on the properties of these complexes.[8]

We discovered earlier that similar to the reaction of [Cu(tmpa)(CH$_3$CN)]$^+$ with O$_2$, the copper(I) complex of the aliphatic ligand Me$_6$tren (= tris(2-dimethylaminoethyl)amine, Scheme 1) also supports the formation of a copper superoxo

---

† Based on the presentation given at Dalton Discussion No. 4, 10–13th January 2002, Kloster Banz, Germany.

DOI: 10.1039/b107927c

Table 1 Crystal data for [Cu(Me_2-uns-penp)(CH_3CN)]ClO_4 (**1**) and [Cu(Me_2-uns-penp)Cl]ClO_4 (**2**)

	1	**2**
Empirical formula	$C_{18}H_{25}ClCuN_5O_4$	$C_{16}H_{22}Cl_2CuN_4O_4$
Formula weight	474.42	468.82
Temperature/K	173(2)	295
Crystal system	Triclinic	Monoclinic
Space group	$P\bar{1}$	$C2/m$
a/Å	7.66920(10)	13.723(1)
b/Å	11.1356(2)	19.224(2)
c/Å	13.1908(2)	7.776(1)
β/°	78.0720(10)	101.90(1)
Volume/Å^3	1037.39(3)	2007.3(3)
Z	2	4
$D_{calc.}$/Mg m^{-3}	1.519	1.551
μ/mm^{-1}	1.216	1.383
F(000)	492	964
Crystal size/mm^3	0.40× 0.35 × 0.30	0.60 × 0.35 × 0.30
Scan technique		ω-scan
θ range for data collection/°	1.94 to 27.47	3.7 to 29.0
Index ranges	$-9 \le h \le 9$, $-14 \le k \le 14$, $-17 \le l \le 17$	$-4 \le h \le 18$, $-4 \le k \le 26$, $-10 \le l \le 10$
Reflections collected	8224	4486
Independent reflections, R_{int}	4737, 0.0174	2756, 0.0237
Observed reflections [$F_o > 4\sigma(F)$]		1931
Data/restraints/parameters	4737/0/362	2756/0/141
Goodness of fit on F^2	1.085	1.047
$R1$ [$F_o > 4\sigma(F)$]	0.0303	0.0478
wR_2 (all data)	0.0924	0.1288
Largest diff. peak and hole/e Å^{-3}	0.376 and −0.498	0.577 and −0.322

and peroxo complex at low temperatures.[3,4,7] In a detailed mechanistic study we observed clear differences in the kinetic behaviour during the oxidation of the two complexes.[25] Therefore, we became interested in the investigation of the copper(I) complexes of the "mixed ligands" Me_2-uns-penp (= (2-dimethylaminoethyl)bis(2-pyridylmethyl)amine) and Me_4-apme (= bis(2-dimethylaminoethyl)(2-pyridylmethyl)amine) shown in Scheme 1. Herein we present our first results on the kinetic investigation of the copper(I) complex [Cu(Me_2-uns-penp)(CH_3CN)]ClO_4 with dioxygen in regard to the application of low temperature stopped-flow techniques and advanced data fitting methods. Further examples of this technique can be found in the literature.[26–35]

Results and discussion

Synthesis and characterization of copper complexes

The copper(I) complex of Me_2-uns-penp was prepared by mixing stoichiometric amounts of the amine and [Cu(CH_3CN)$_4$]ClO_4 in acetonitrile under argon. An ORTEP[55] plot of the cation of [Cu(Me_2-uns-penp)(CH_3CN)]ClO_4 (**1**) is shown in Fig. 1 and a summary of the crystallographic data and refinement parameters can be found in Table 1. Selected bond lengths and angles are reported in Table 2.

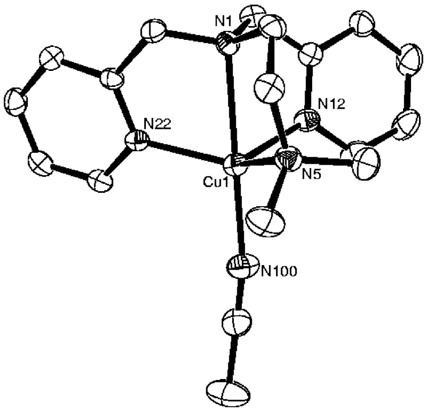

Fig. 1 View of the cation of [Cu(Me_2-uns-penp)(CH_3CN)]ClO_4.

As discussed above, the ligand Me_2-uns-penp can be regarded as a "mixture" of the two ligands tmpa and Me_6tren and therefore a comparison of the crystal structures of the copper complexes of these ligands with [Cu(Me_2-uns-penp)(CH_3CN)]ClO_4 is interesting. [Cu(tmpa)(CH_3CN)]$^+$ crystallizes in the same way as [Cu(Me_2-uns-penp)(CH_3CN)]$^+$ with an acetonitrile molecule as additional ligand in the axial site (Cu–N: 1.99(1) Å in [Cu(tmpa)(CH_3CN)]$^+$,[36] Cu–N: 2.038(2) Å in [Cu(Me_2-uns-penp)(CH_3CN)]$^+$). The coordination geometry of both complexes is best described as slightly distorted trigonal bipyramidal. The copper(I) ion is displaced 0.508 Å out of the N5–N12–N22 trigonal plane in [Cu(Me_2-uns-penp)(CH_3CN)]$^+$ and 0.55 Å in [Cu(tmpa)(CH_3CN)]$^+$.

In contrast, the copper(I) complex of Me_6tren shows a quite different crystal structure.[4] Here no acetonitrile molecule is coordinated in the solid state, however, a perchlorate ion shows a weak interaction with the copper ion. The copper ion in [Cu(Me_6tren)]$^+$ only lies slightly below the trigonal plane (0.191(8) Å) towards the perchlorate ion. The reason for this is that the soft aromatic nitrogen atoms of the pyridines form stronger bonds with the soft copper(I) ion than the hard aliphatic amine donor atoms. As a result the bond lengths to the axial and the equatorial nitrogens in [Cu(Me_6tren)]$^+$ are very similar (2.122(7) and 2.200(14) Å) in contrast to the other two complexes where the bond length to axial nitrogen is significantly longer (Cu–N_{axial} = 2.424(2) Å and Cu–$N_{equ.}$ = 2.061(2)–2.208(2) Å). Therefore, the crystal structure of [Cu(Me_2-uns-penp)(CH_3CN)]$^+$ more closely resembles the structure of [Cu(tmpa)(CH_3CN)]$^+$ than that of [Cu(Me_6tren)]$^+$.

The copper(II) complex [Cu(Me_2-uns-penp)Cl]ClO_4 (**2**) was prepared by mixing stoichiometric amounts of $Cu(ClO_4)_2\cdot 6H_2O$, $CuCl_2\cdot 2H_2O$ and Me_2-uns-penp in a mixture of methanol and water (1 : 1). A summary of crystal parameters and refinement results for this compound is given in Table 1. An ORTEP plot of this complex is presented in Fig. 2 with selected bond distances and angles in Table 2.

The molecule is situated on a crystallographic mirror plane and the coordination geometry is best described as distorted square pyramidal. This is surprising because the related complexes [Cu(tmpa)Cl]ClO_4 and [Cu(Me_6-tren)Cl]ClO_4 are both trigonal bipyramidal in the solid state.

The square pyramidal geometry is not completely retained

Table 2 Selected bond distances (Å) and angles (°) for [Cu(Me$_2$-uns-penp)(CH$_3$CN)]ClO$_4$ (**1**) and [Cu(Me$_2$-uns-penp)Cl]ClO$_4$ (**2**)

1			
Cu(1)–N(1)	2.4236(14)	Cu(1)–N(22)	2.0613(14)
Cu(1)–N(5)	2.2608(15)	Cu(1)–N(100)	2.0380(17)
Cu(1)–N(12)	2.0932(15)		
N(1)–Cu(1)–N(5)	76.53(5)	N(5)–Cu(1)–N(22)	124.98(5)
N(1)–Cu(1)–N(12)	76.10(5)	N(5)–Cu(1)–N(100)	97.76(6)
N(1)–Cu(1)–N(22)	76.04(5)	N(12)–Cu(1)–N(22)	116.46(6)
N(1)–Cu(1)–N(100)	173.79(6)	N(12)–Cu(1)–N(100)	107.76(7)
N(5)–Cu(1)–N(12)	101.64(5)	N(22)–Cu(1)–N(100)	105.86(6)
2			
Cu(1)–N(1)	2.320(3)	Cu(1)–N(3)A	2.000(3)
Cu(1)–N(2)	2.058(3)	Cu(1)–Cl(1)	2.252(2)
Cu(1)–N(3)	2.000(3)		
N(1)– Cu(1)–N(2)	83.94(13)	N(2)–Cu(1)–N(3)A	82.67(7)
N(1)–Cu(1)–N(3)	96.32(7)	N(2)–Cu(1)–Cl(1)	175.12(10)
N(1)–Cu(1)–N(3)A	96.32(7)	N(3)–Cu(1)–N(3)A	159.5(2)
N(1)–Cu(1)–Cl(1)	100.94(9)	N(3)–Cu(1)–Cl(1)	96.69(7)
N(2)–Cu(1)–N(3)	82.67(7)	N(3)A–Cu(1)–Cl(1)	96.69(7)

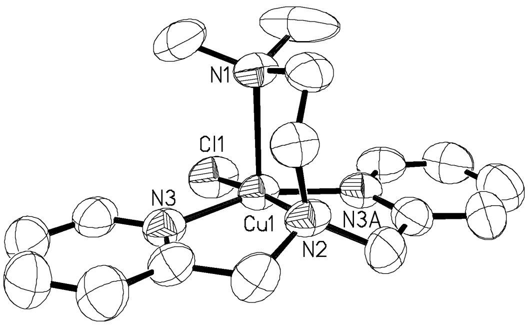

Fig. 2 View of the cation of [Cu(Me$_2$-uns-penp)Cl]ClO$_4$.

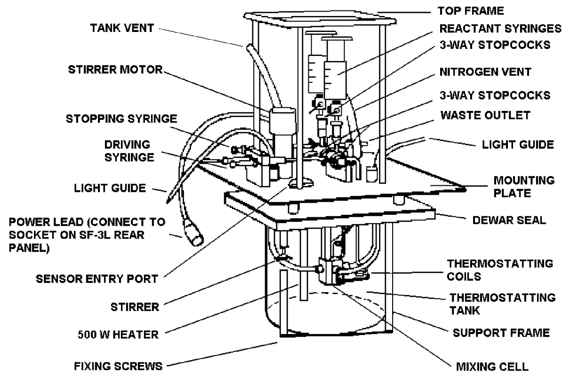

Fig. 3 Low temperature stopped-flow module.

in solution because in the UV-vis spectrum a very broad band with an absorbance maximum at 780 nm was observed. Square pyramidal complexes typically have an absorbance maximum around 650 nm while for trigonal bipyramidal copper complexes absorbance maxima between 850 and 900 nm are observed.[37,38]

The low temperature stopped-flow technique

Recently, "copper dioxygen adducts" have been reported which are quite stable at room temperature.[39–42] Commonly such compounds formed by the reaction of copper(I) complexes with dioxygen are stable only at low temperatures.[7,10,24,39] Typically, for copper(I) complexes these reactions are usually quite fast and need to be investigated using stopped-flow techniques.[7,10,24] As a consequence several problems need to be overcome in order to successfully study the kinetics of these reactions. The instrument must allow measurements at temperatures as low as −100 °C to be possible and simultaneously the connection and tubing system has to be air tight and prevent the leaking of the cooling media into the solutions of the reactants. Sealings, O-rings, *etc.*, are especially vulnerable because of the effects of organic solvents and the large temperature changes involved. Stopped-flow instruments commercially available today do not incorporate these features and therefore need to be modified to perform such kinetic studies. Unfortunately these modifications usually do not allow work below temperatures of −40 °C. The low temperature stopped-flow instrument SF-40 (latest model number) manufactured by Hi-Tech Scientific (based on an original design by Caldin, Crooks and Queen)[43] suitable for such measurements is, however, no longer commercially available due to its production being stopped recently.

In our laboratory we employ a modified Hi-Tech SF-3 L low temperature stopped-flow unit (Fig. 3). In the original instrument only glass was used as the material for the syringes, all tubing and connections. This avoided almost completely the contact of the solutions with air (only a very small risk of air contamination remained at the valves of the syringes). This setup has been used successfully for many years by Zuberbühler and coworkers. Later on Hi-Tech Scientific replaced the glass connections with Teflon tubing. This reduced the risk of glass breaking but introduced the problem of oxygen diffusion through the Teflon tubes. In the beginning of our investigations our instrument was equipped with such Teflon tubing and, being aware of this problem, we tried to exclude contamination with dioxygen in different ways. We could successfully follow the oxidations of the copper(I) complexes with dioxygen, but we had to learn that diffusion of air into the system still could not be completely avoided. This was extremely unfortunate because as a consequence it was not possible to perform quantitative kinetic studies with this instrument. Therefore (in cooperation with the company J&M, Aalen, Germany) we decided to replace the Teflon tubing by glass in a different manner than in the original instrument.

On top of the stopped flow unit commercially available 5 ml glass syringes (Fortuna Optima, Graf & Co. GmbH, Wertheim, Germany) are connected by three-way Hamilton valves (Hamilton Company, Reno, NV, USA) to the glass tubes which then spiral downwards to the cuvette. Between the glass tubing and the optical 1 cm quartz cuvette (specially manufactured for this instrument by Hellma GmbH & Co. KG, Müllheim, Germany) a mixing jet is installed. The connections are made tight with O-rings and flexible light fibers (J&M) are attached with Teflon sealings at the cuvette. With this setup contamination of the solutions with dioxygen can be completely avoided. An excellent test for the system was our kinetic investigation of the reactions of the extremely dioxygen sensitive Ni(O) complex [(bipy)Ni(COD)] with unsaturated substrates.[26] A possible alternative to the glass tubing for anaerobic measurements had been introduced by Hi-Tech earlier, using either stainless steel or Teflon coated stainless steel tubing. Here dioxygen contamination can also be excluded completely after the oxygen in the tubing reacted (this setup has been used successfully by other research groups).[27,35]

The two glass coils and the mixing chamber with the cuvette are immersed in an ethanol bath which is placed in a Dewar that is filled with liquid nitrogen for low temperature measurements. The ethanol bath is cooled by liquid nitrogen evaporation, and its temperature is measured by using a Pt resistance thermometer and can be maintained to within ±0.1 °C using a temperature-controlled thyristor power unit (both Hi-Tech). With our diode array instrumentation complete spectra can be collected between 190 and 620 nm or 350 and 1100 nm (both J&M).

At this point it should be pointed out that there are alternatives for the diode array instrumentation: for example automatic repetitive measurements (scanning over each single wavelength in a selected range) can be performed using an Applied Photophysics Ltd. stopped-flow instrument. Most of the time the diode array technique is superior to these alternatives but a problem can arise if photochemistry is observed (filters can be used in some cases to suppress this).[5,44]

Furthermore, it is worthwhile mentioning that it is possible to perform stopped-flow measurements at low temperatures and high pressures. However, it is a challenging task to study dioxygen sensitive samples under these conditions.[5,45]

As dilute solutions of the copper(I) complexes are very reactive towards dioxygen, solutions for the kinetic measurements (usually 0.1–0.5 mM) were always prepared in an argon glove box. Transfer of these solutions to the stopped-flow unit was achieved by using 50 ml glass syringes (Fortuna Optima) connected to a three-way Hamilton valve. No leakage of dioxygen into the solutions in the syringes was observed. Rinsing the instrument 3 to 4 times with the complex solution prior to the measurements allowed the removal of all the remaining oxygen.

Saturated solutions of dioxygen were obtained by bubbling dioxygen through the required solvent for about 20 minutes (while avoiding contamination with water) and then thermostatting the solution at 20 °C.[23] The solution can then be transferred to the stopped-flow instrument in a syringe with a Hamilton valve. Dilution was accomplished by mixing the dioxygen saturated solvent with the argon saturated solvent, with the two syringes being connected by Hamilton valves. Alternatively a gas mixing setup could be used.[34] Air saturation has been used in the past to obtain lower concentrations of dioxygen but here it should be made certain that no reaction of the reactants with carbon dioxide or nitrogen can occur.[23]

Kinetic data are obtained by measuring absorbance *vs.* time data at a single wavelength or, much more preferable (especially for more complex systems like the one described herein; see below), by obtaining complete time resolved spectra using a diode array system. Modern diode array systems allow a full spectrum to be recorded every 0.8 ms. For our studies we use a system from J&M.

The analysis of the reaction of [Cu(Me_2-uns-penp)(CH_3CN)]ClO_4 with dioxygen

To illustrate the data collection with such a low temperature stopped-flow unit, the reaction of [Cu(Me_2-uns-penp)(CH_3CN)]ClO_4 with dioxygen is presented below.[46] Time resolved spectra of this reaction in propionitrile at −90.1 °C are shown in Fig. 4. These spectra provide clear evidence for the formation of superoxo and peroxo complexes because the spectral features are very similar to the UV-vis spectra of the copper superoxo and peroxo complexes of the parent ligands tmpa and Me_6tren.[4,23] We assigned the absorbance maxima of the superoxo [(Me_2-uns-penp)CuO_2]$^+$ (λ_{max} = 412 nm) and peroxo [(Me_2-uns-penp)CuO_2Cu(Me_2-uns-penp)]$^{2+}$ (λ_{max} = 528 nm) complexes accordingly.

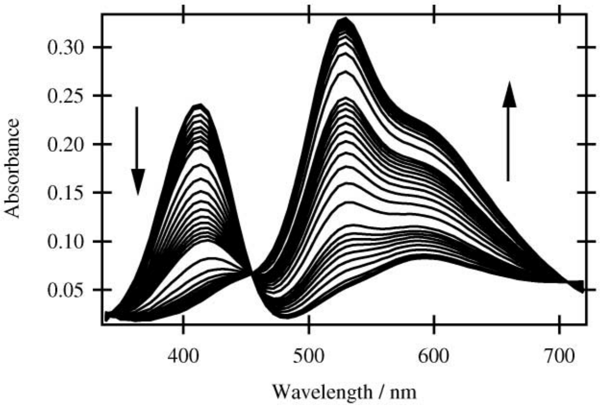

Fig. 4 Time resolved spectra of the reaction of [Cu(Me_2-uns-penp)(CH_3CN)]PF_6 with dioxygen in propionitrile at −90.1 °C ([complex] = 2.44×10^{-4} M, [O_2] = 4.4×10^{-3} M, total time = 149.83 s, four time bases (number of measurements 20/50/80/106, number of intermissions 0/20/100/1000), integration time = 1.3 ms). Only every seventh spectrum is shown.

Even at −90.1 °C the formation of [(Me_2-uns-penp)CuO_2]$^+$ is too fast to be followed spectroscopically under these conditions. Only very few spectra showing the increase of the absorbance at 412 nm can be obtained using very short overall reaction times (0.33 s) and therefore the majority of this reaction is missing during the measurement. In contrast the formation of [(Me_2-uns-penp)CuO_2Cu(Me_2-uns-penp)]$^{2+}$ can be followed nicely by observing the increase of the absorbance maximum at 528 nm.

This increase is accompanied by the decrease of the absorbance of the superoxo complex at 412 nm. The reaction pathway follows eqns. (1)–(3) as described previously for [(tmpa)Cu(CH_3CN)]$^+$ and [Cu(Me_6tren)(CH_3CN)]$^+$ (R = CH_3, C_2H_5; L = tripodal ligand).[4,23]

$$[(L)Cu(RCN)]^+ + O_2 \underset{k_{-1}}{\overset{k_1}{\rightleftharpoons}} [(L)Cu(O_2)]^+ + RCN \qquad (1)$$

$$[(L)Cu(RCN)]^+ + [(L)Cu(O_2)]^+ \underset{k_{-2}}{\overset{k_2}{\rightleftharpoons}} [(L)Cu(O_2)Cu(L)]^{2+} + RCN \qquad (2)$$

$$[(L)Cu(O_2)Cu(L)]^{2+} \longrightarrow \text{irreversible decay} \qquad (3)$$

A comparison of the stability of the peroxo complexes [(Me_2-uns-penp)CuO_2Cu(Me_2-uns-penp)]$^{2+}$, [(tmpa)CuO_2Cu(tmpa)]$^{2+}$ and [(Me_6tren)CuO_2Cu(Me_6tren)]$^{2+}$ clearly shows that, interestingly enough, [(Me_2-uns-penp)CuO_2Cu(Me_2-uns-penp)]$^{2+}$ is more persistent at higher temperatures in contrast to the other two peroxo complexes. As shown in Fig. 5a [(Me_2-uns-penp)CuO_2Cu(Me_2-uns-penp)]$^{2+}$ is still observable at 5 °C for a few minutes in contrast to [(tmpa)CuO_2Cu(tmpa)]$^{2+}$ (Fig. 5b). [(Me_6tren)CuO_2Cu(Me_6tren)]$^{2+}$ is stable for a few seconds under these conditions.

Prior to the experiment we expected to find the stability of the peroxo complexes in the order of [(Me_6tren)CuO_2Cu(Me_6tren)]$^{2+}$ > [(Me_2-uns-penp)CuO_2Cu(Me_2-uns-penp)]$^{2+}$ > [(tmpa)CuO_2Cu(tmpa)]$^{2+}$. An explanation for the fact that [(Me_2-uns-penp)CuO_2Cu(Me_2-uns-penp)]$^{2+}$ is more persistent at higher temperatures than the other two peroxo complexes might be a consequence of their different geometries. In contrast to the trigonal bipyramidal geometries of [(tmpa)CuO_2Cu(tmpa)]$^{2+}$ and [(Me_6tren)CuO_2Cu(Me_6tren)]$^{2+}$ with the peroxo ligand occupying the axial position, the geometry of [(Me_2-uns-penp)CuO_2Cu(Me_2-uns-penp)]$^{2+}$ is distorted square pyramidal with the peroxo ligand occupying an equatorial position. No crystal structure of the peroxo complex is available

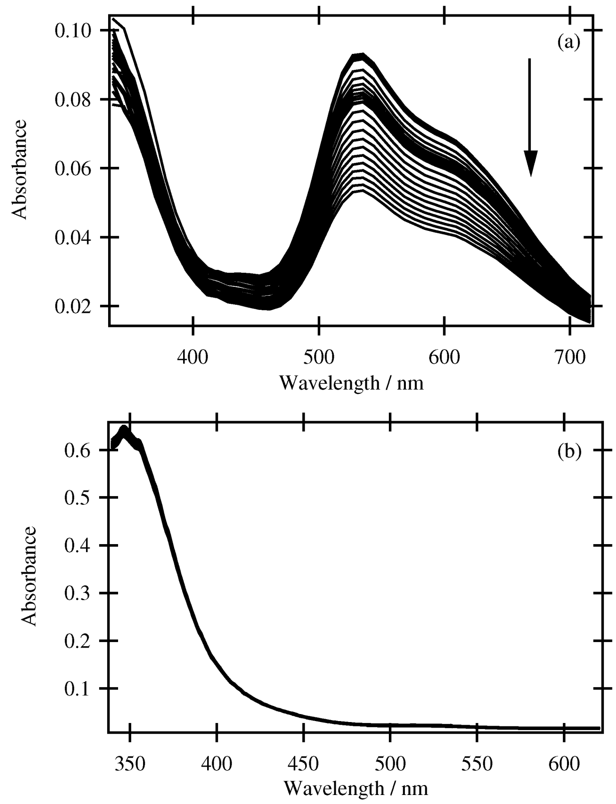

Fig. 5 (a) Time resolved spectra of the reaction of [Cu(Me$_2$-uns-penp)(CH$_3$CN)]PF$_6$ with dioxygen in propionitrile at +4.9 °C ([complex] = 2.44 × 10^{-4} M, [O$_2$] = 4.4 × 10^{-3} M, total time = 177.66 s, four time bases (number of measurements 20/40/80/116, number of intermissions 0/10/250/1000), integration time = 1.3 ms). Only every tenth spectrum is shown. (b) Time resolved spectra of the reaction of [Cu(tmpa)(CH$_3$CN)]ClO$_4$ with dioxygen in propionitrile at +5.1 °C ([complex] = 2.0 × 10^{-4} M, [O$_2$] = 4.4 × 10^{-3} M, total time = 177.66 s, one time bases (number of measurements 256), integration time = 2.0 ms). Only every seventh spectrum is shown.

to date but the structure can be inferred from [Cu(Me$_2$-uns-penp)Cl]ClO$_4$ (described above) as has been shown for copper tmpa complexes.[4,21–23] This structural difference is important because a peroxo ligand in the axial position of a square pyramidal copper complex would be very labile towards substitution. Most likely for this reason we could not detect oxygenation intermediates spectroscopically during the oxidation of [Cu(trien)]$^+$, where the peroxo ligand would be axially coordinated in a square pyramidal product complex.[6]

Further support for this explanation comes from the fact that oxygenation of copper(I) complexes with bispidine-type ligands leads to unusually stable end-on μ-peroxo dicopper(II) compounds. Bispidine-type ligands are very rigid and enforce a square-pyramidal structure with the additional ligand being coordinated in an equatorial position.[39]

Application of global analysis for data fitting

The investigation of the reactions of these tripodal copper(I) complexes with dioxygen not only requires sophisticated techniques for the actual measurements (as illustrated above) but also the analysis of the kinetic data is only possible by using advanced data fitting methods. This is a consequence of the combined consecutive equilibrium reactions (eqns. (1)–(3)). Today the majority of researchers still use the method of fitting data with exponential functions by the application of iterative fitting procedures.[47] For example the first step (eqn. (1)) in the reaction scheme described above is the formation of a superoxo complex. Using pseudo-first order conditions ([O$_2$] ≫ [copper(I) complex]) leads to the simple rate law:

$$\text{d[superoxo complex]/d}t = k_{\text{obs}} \times \text{[copper(I) complex]}$$

and absorbance *vs.* time traces can be fitted to a single exponential function using programs such as Igor or Origin. These programs immediately calculate k_{obs} and also provide information on the goodness of fit (plots of the residuals). Methods that linearize the kinetic data by log plots instead of the iterative methods are still applied but are much less accurate and should no longer be used.[47] According to eqn. (1) a plot of k_{obs} *vs.* [O$_2$] would allow the calculation of the second order rate constant for the forward reaction from the slope and the first order rate constant for the back reaction from the intercept. In principle this approach could be used for the reaction of [Cu(Me$_2$-uns-penp)(CH$_3$CN)]ClO$_4$ with dioxygen. Unfortunately the formation of the superoxo complex is too fast to be followed spectroscopically under these conditions (this fitting method has been nicely described for the reaction of cobalt(II) complexes with dioxygen[34]).

However, while the approach of using exponential functions (to fit absorbance *vs.* time traces at single wavelengths) could be applied to the formation of the superoxo complex this is no longer possible for the formation of the peroxo complexes. In this case a global analysis fitting routine is necessary and programs specifically suitable for the analysis of kinetic data have been commercially available for some years, often distributed together with a stopped-flow instrument (Pro/Kineticist (Applied Photophysics Ltd.), SPECFIT (Hi-Tech Scientific)). These programs represent a major advance in the capability of data analysis and are extremely powerful. Their application in kinetic studies is highly recommended. Most importantly they allow one to globally analyse the complete set of wavelength/absorbance/time data according to a proposed reaction scheme. The mathematical background of these programs is described in detail in the literature.[48–52] In the following the fitting procedure with SPECFIT/32 (authors R. A. Binstead, B. Jung and A. D. Zuberbühler) is illustrated (Pro/Kineticist is based on the same mathematical routines).

As discussed in the Introduction only recently has instrumentation become available for generating high quality sets of time dependent spectra comprising of many thousands of individual absorbance measurements. For stopped-flow kinetics the use of this method only became possible due to the improvement of diode array instrumentation, as discussed above, allowing these data to be obtained on a very fast time scale. SPECFIT provides the global analysis of equilibrium and kinetic systems with expanded SVD (singular value decomposition) and non-linear regression modelling by the Levenberg–Marquardt method.[48–52] These fitting routines make it possible to fully analyse complete data sets.

During the global analysis the non-linear reaction parameters (rates) at all measured wavelengths are simultaneously optimised. Herein individual rates contribute to each kinetic record to a different degree over the measured wavelength range and the global analysis of all records reduces the correlation of these parameters (see below). This allows one to fully analyse all data according to a proposed reaction scheme and a reliable identification of minor intermediates. In addition spectra of transient intermediates can be calculated.

The procedure of data fitting generally starts by importing all measured data into the program (for example data obtained for the measurements shown in Fig. 4). The import menu provides access to a number of instrument-specific file import converters, and in addition, there are different ASCII file converters for both ASCII XY (single scan) and specialized ASCII XYZ spreadsheet (multi-scan) file converters to import multi-wavelength scans from unsupported data sources. Typically such data sets consist of individual scans from a spectrophotometer (UV-vis, FTIR *etc.*) that have been collected as a function of time. In kinetic studies, SPECFIT provides specialized procedures to import diode array and rapid-scan spectra from the most commonly used stopped-flow kinetic spectrometers.

The SVD procedure can be carried out during the process of the file import. The user provides additional information (*e.g.* concentration of reactants, nature of the solvent *etc.*) either for each individual file or for a complete file series. Furthermore, the program calculates automatically the correct concentrations of the reactants according to the density corrections at low temperatures.

Experimental 3D data sets obtained in such a manner contain measurements at many more wavelengths than the number of coloured components that are represented by the colourimetric changes for the equilibrium or kinetic system under study. The goal of the data reduction procedure is to determine a solution for Beer's Law,

$$A = C \times E$$

where

A = matrix of experimental absorbance readings $N_m \times N_w$)
C = matrix of calculated concentration profiles ($N_m \times N_c$)
E = matrix of molar absorptivity spectra ($N_c \times N_w$)

and

N_c = number of coloured species
N_m = number of measurements
N_w = number of wavelengths in scans

This is an example of an over-determined system of linear equations, which has no unique mathematical solution. Therefore, it is necessary to employ special methods in order to solve simultaneously for both unknown spectra and concentration profiles. For this the singular value decomposition (SVD) matrix methodology is used to obtain a basis set of eigenvectors, whose matrix product Y' ($U \times S$ = concentration eigenvectors; S = diagonal matrix, whose elements are the square roots of the Eigenvalues; V = spectroscopic eigenvector):

$$Y' = U \times S \times V$$

is the least-squares best estimator of the original 3D data set (Y). The SVD method produces a linearly independent set of eigenvectors with all of the colourimetric information for the experiment, plus some additional noise eigenvectors, that can be excluded from further consideration. The matrix product ($U \times S$) contains the information of the coloured components and they are often called the *concentration eigenvectors* which are used as the input data for the global fitting procedure. If the number of significant eigenvectors is known (which represent the number of coloured species), it is much easier to enter a certain kinetic model.

The prediction of relevant eigenvectors should only be used as a guide. To ensure that the number of calculated eigenvectors is correct, the plots of the eigenvectors are normally more definitive. A relevant eigenvector should show a structured behaviour, while a non-relevant eigenvector only shows statistical noise. For the example of the reaction of [Cu(Me$_2$-uns-penp)(CH$_3$CN)]ClO$_4$ with dioxygen we observed two relevant eigenvectors at −90.1 °C (shown in Fig. 6). All the other eigenvectors are non-relevant and only show statistical noise (only one of these is shown in Fig. 6). Two relevant eigenvectors in our example mean that the decay of the species [Cu(Me$_2$-uns-penp)(CH$_3$CN)]ClO$_4$ has been completed within the mixing time and only the superoxo- and peroxo-complex are involved in the observed reaction under these conditions.

The Kinetic Model Editor menu provides a group of controls that allow the user to define complex kinetic models in the form of elementary reaction steps. The reactions are entered in a manner that is familiar to chemists (*e.g.*, A + B ⟶ C) and are automatically translated to differential equations as each equation is completed. For our example the complete reaction scheme is given by:

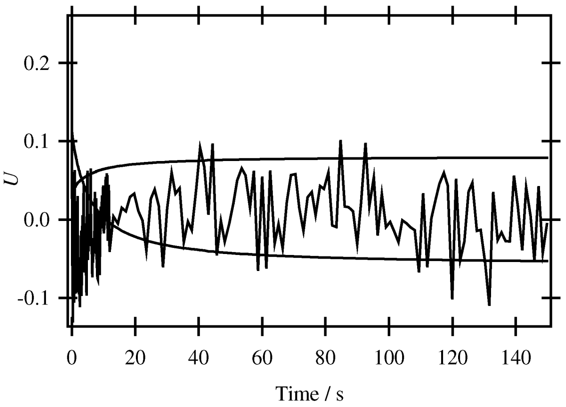

Fig. 6 Plot of the eigenvectors *vs.* time.

$$\mathrm{A + B \longrightarrow C} \quad \text{(a)}$$

$$\mathrm{C \longrightarrow A + B} \quad \text{(b)}$$

$$\mathrm{A + C \longrightarrow D} \quad \text{(c)}$$

$$\mathrm{D \longrightarrow A + C} \quad \text{(d)}$$

$$\mathrm{D \longrightarrow E} \quad \text{(e)}$$

Calculations for the present kinetic experiments are based on this scheme, with one or more simplifications, depending on the experimental observations. Some of the kinetic parameters can only be calculated in a restricted temperature range. Outside the range, either extrapolated values may have to be used or the mechanistic model scheme may be appropriately simplified as discussed earlier for the [Cu(tmpa)(CH$_3$CN)]$^+$ system.[23]

Furthermore, information is provided here by the user as to whether the species is coloured or not. If the spectrum of an intermediate is known, the fixed spectrum of this compound will be used in the calculation. The resulting system of differential rate equations will be solved *via* numerical integration methods (rate constants can be fixed or variable). After the fit is performed according to the model, the results of the calculation can be compared to the measured data (the correctness of the model can then be either confirmed or proven incorrect). For our example of the reaction of [Cu(Me$_2$-uns-penp)(CH$_3$CN)]ClO$_4$ with dioxygen at −90.1 °C only eqns. (a)–(d) need to be used (decomposition of the peroxo complex according to eqn. (e) is not relevant under these conditions). Measured data and the fit together with the residuals for the absorbance *vs.* time traces at 412 and 528 nm are shown in Figs. 7a and b. They clearly demonstrate the goodness of the fit according to the model used.

Rate constants for the fit according to the model described above were calculated to be: $k_1 = 1.5 \times 10^3$ M^{-1} s^{-1}, $k_{-1} = 1.2$ s^{-1}, $k_2 = 2.6 \times 10^3$ M^{-1} s^{-1} and $k_{-2} = 1.0 \times 10^{-4}$ s^{-1} (see eqns. (1) and (2)).[46] These values compare well with the results for the copper(I) tmpa system (see below) and the preliminary rate constants obtained for the reaction of [Cu(Me$_6$tren)(CH$_3$CN)]$^+$ with dioxygen ($k_1 = 9.4 \times 10^4$ M^{-1} s^{-1}, $k_{-1} = 0.07$ s^{-1}, $k_2 = 1.5 \times 10^4$ M^{-1} s^{-1} and $k_{-2} = 5.4 \times 10^{-5}$ s^{-1}).[25] However, it should be pointed out that Zuberbühler and coworkers strongly discourage comparisons of kinetic or equilibrium constants at a given temperature because these can sometimes be very misleading.[23,53] Therefore, discussion of activation or thermodynamic parameters should be preferred wherever possible.[23,25,46,53]

For a complete analysis of such a kinetic system more than a hundred time resolved spectra at different temperatures and concentrations need to be recorded and analysed.[23] This allows the calculation of the rate constants and the activation parameters for all individual steps. Furthermore, the equilibrium

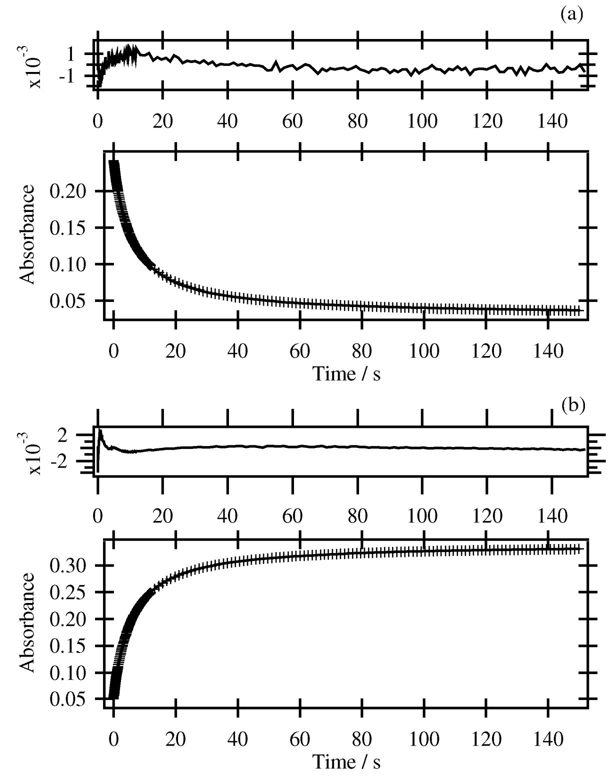

Fig. 7 (a) Measured data (+), fit (solid line) and residuals for the absorbance *vs.* time trace at 412 nm. (b) Measured data (+), fit (solid line) and residuals for the absorbance *vs.* time trace at 528 nm.

constants can be derived for the reactions shown in eqns. (1) and (2). So far, there are only a few systems analysed in such a detailed way, *e.g.* the reaction of $[(tmpa)Cu(CH_3CN)]^+$ with dioxygen.[23,53] The kinetic and thermodynamic results for this reaction (obtained by a low temperature stopped-flow study using global analysis fitting methods) are presented in Table 3. A good overview on the kinetics and thermodynamics of copper(I)–dioxygen interaction has been reported earlier by Karlin, Kaderli and Zuberbühler.[53]

Summary

The advances in low temperature stopped-flow techniques (together with diode array instrumentation) as well as in computer programs for data fitting (using numerical integration methods, and factor analysis) have enabled deduction of multistep complex kinetic mechanisms of reactions that are too fast at ambient temperatures. This includes determination of kinetic and thermodynamic parameters and elucidation of complete UV-vis spectra of reactive intermediates that can only be observed at low temperatures.

To illustrate this method we have described herein the investigation of the reaction of $[Cu(Me_2\text{-uns-penp})(CH_3CN)]ClO_4$ with dioxygen. Clear differences between this reaction and the analogous oxidation of $[Cu(Me_6tren)]ClO_4$ and $[Cu(tmpa)(CH_3CN)]ClO_4$ were observed. Interestingly enough, it was found that $[(Me_2\text{-uns-penp})CuO_2Cu(Me_2\text{-uns-penp})]^{2+}$ is more persistent at higher temperatures than the peroxo complexes obtained from the other two copper(I) complexes. This might be a consequence of their different geometries as discussed above.

Experimental

General

Table 3 Kinetic and thermodynamic parameters for the reaction of O_2 with $[(tmpa)Cu(CH_3CN)]^+$ [23,53]

Parameter	183 K	298 K
k_1/M^{-1} s^{-1}	$(1.8 \pm 0.1) \times 10^4$	8×10^7
$\Delta H^\#$/kJ mol^{-1}	32 ± 4	
$\Delta S^\#$/J K^{-1} mol^{-1}	14 ± 18	
k_{-1}/s^{-1}	8 ± 1	2×10^8
$\Delta H^\#$/kJ mol^{-1}	66 ± 4	
$\Delta S^\#$/J K^{-1} mol^{-1}	137 ± 18	
k_2/M^{-1} s^{-1}	$(3.2 \pm 0.2) \times 10^4$	$(1.8 \pm 0.1) \times 10^6$
$\Delta H^\#$/kJ mol^{-1}	14 ± 1	
$\Delta S^\#$/J K^{-1} mol^{-1}	-78 ± 2	
k_{-2}/s^{-1}	$(1.5 \pm 0.8) \times 10^{-4}$	$(1.2 \pm 0.3) \times 10^3$
$\Delta H^\#$/kJ mol^{-1}	14 ± 1	
$\Delta S^\#$/J K^{-1} mol^{-1}	-78 ± 2	
K_1/M^{-1}	$(1.9 \pm 0.1) \times 10^3$	(0.34 ± 0.08)
ΔH^0/kJ mol^{-1}	-34 ± 1	
ΔS^0/J K^{-1} mol^{-1}	-123 ± 4	
K_2/M^{-1}	$(2.2 \pm 0.7) \times 10^8$	$(1.5 \pm 0.4) \times 10^3$
ΔH^0/kJ mol^{-1}	-47 ± 3	
ΔS^0/J K^{-1} mol^{-1}	-97 ± 10	

Preparation and handling of air-sensitive compounds was carried out in a glove box filled with argon (Braun, Garching, Germany; water and dioxygen less than 1 ppm). Synthesis and characterization of $[Cu(tmpa)(CH_3CN)]ClO_4$ is described elsewhere.[22] The ^{1}H-NMR measurements were recorded on a Bruker DXP 300 AVANCE spectrometer. Elemental analyses were performed on a Carlo-Erba Element Analyzer (type 1106) at the University of Erlangen-Nürnberg. The amine uns-penp was synthesized according to the literature.[54]

CAUTION: Perchlorate salts of metal complexes are potentially explosive and should be handled with care.

Syntheses

Me_2-uns-penp. The ligand was obtained by a reductive methylation of the amine uns-penp. To uns-penp (4 g, 16.5 mmol) in a flask a 98% solution of formic acid (25 ml, 0.66 mol) and a 38% solution of formaldehyde (15 ml, 0.54 mol) were added. The solution was stirred at 80 °C for 5 hours and the stirring was continued without heating overnight. HCl was added until pH 2 was reached and the volume of the solution was reduced to dryness. The residue was dissolved in a small amount of water and NaOH (25%) was added until a pH of 11 was reached. The solution was then extracted with CH_2Cl_2, and after drying over Na_2SO_4 the solvent was removed on a rotary evaporator. The crude product was obtained as a dark brown viscous liquid. The amine was further purified by column chromatography (alumina) with ethyl acetate–methanol (9 : 1) yielding a brown oil in 55% yield. ^{1}H-NMR ($CDCl_3$): δ 8.54–7.12 (m, 8 H, aromatic), 3.83 (s, 4 H, methylene), 2.7 (t, 2 H, $-CH_2-CH_2-NMe_2$), 2.5 (t, 2 H, $-CH_2-CH_2-NMe_2$), 2.18 (s, 6 H, $-CH_3$)

$[Cu(Me_2\text{-uns-penp})(CH_3CN)]ClO_4$. $[Cu(CH_3CN)_4]ClO_4$ (0.18 g, 0.55 mmol) was added with stirring to a solution of Me_2-uns-penp (0.15 g, 0.55 mmol) in a small amount of acetonitrile under argon. A large amount of diethyl ether was added to the orange solution to precipitate the complex. The solution was filtered through a medium porosity frit, and the solid was washed with diethyl ether. The yellow powder was dissolved in a small amount of acetonitrile. Crystals suitable for structural characterization were obtained by diffusion of diethyl ether into this solution (yield: 0.1 g, 40%). Anal. calcd. for $C_{18}H_{25}ClCuN_5O_4$: C, 45.57; H, 5.31; N, 14.76. Found: C, 45.77; H, 5.50; N, 14.65%.

$[Cu(Me_2\text{-uns-penp})Cl]ClO_4$. To a solution of Me_2-uns-penp (0.45 g, 1.66 mmol) in 15 ml of methanol was added a solution of $Cu(ClO_4)2{\cdot}6\ H_2O$ (0.31 g, 0.83 mmol) and $CuCl_2{\cdot}2\ H_2O$ (0.14 g, 0.83 mmol) in 10 ml of water. The solution was stirred for 10 min and filtered. After the recrystallization of the crude product from methanol blue crystals formed which were suitable for structural characterization (yield: 0.54 g, 70%). Anal. calcd. for $C_{16}H_{22}Cl_2CuN_4O_4$: C, 40.99; H, 4.73; N, 11.95. Found: C, 41.07; H, 4.91; N, 11.89%.

Kinetic measurements

Propionitrile used for the kinetic measurements was purified according to published procedures. Preparation and handling of air-sensitive compounds was carried out in a glove box. Dioxygen saturated solutions for the kinetic measurements were obtained by bubbling dioxygen (Linde, Germany) through the solvent for 20 minutes as described earlier (solubility of dioxygen in propionitrile is $(8.8 \pm 1.0) \times 10^{-3}$ M atm^{-1}).[23] Time resolved spectra of the reactions of dioxygen with copper(I) complexes were recorded on a modified Hi-Tech SF-3 L low temperature stopped-flow unit (Hi-Tech, Salisbury, UK) equipped with a J&M TIDAS 16–500 diode array spectrophotometer (J&M, Aalen, Germany) as described above. Data fitting was performed using the integrated J&M software Kinspec, Origin (OriginLab Corporation, Northampton, MA, USA) or Igor (WaveMetrics, Inc., Lake Oswego, OR, USA) for simple exponential functions or the program Specfit (Spectrum Software Associates, Marlborough, MA 01752, USA) as discussed above.

Crystal structure analyses

Crystal data and experimental conditions for the two complexes are listed in Table 1. The molecular structures are illustrated in Figs. 1 and 2. Selected bond lengths and angles with standard deviations in parentheses are presented in Table 2. Three-dimensional X-ray data were collected either on a Nonius-KappaCCD (**1**) or on a Siemens P4 diffractometer (**2**) using graphite monochromated Mo-Kα radiation (λ = 0.71069 Å). Single crystals were coated with polyfluoroether oil and mounted on a glass fiber. Lorentz, polarization, and empirical absorption corrections were applied. Space groups were determined from systematic absences and subsequent least-squares refinement. The structures were solved by direct methods. The parameters were refined using SHELXTL 5.03.[56] Non-hydrogen atoms were refined with anisotropic thermal parameters. The hydrogen atoms were localized and isotropically refined for **1** and fixed in idealized positions using a riding model for **2**.

CCDC reference numbers 173001 and 173002.

See http://www.rsc.org/suppdata/dt/b1/b107927c/ for crystallographic data in CIF or other electronic format.

Acknowledgements

The authors gratefully acknowledge financial support from the DFG. Furthermore, they thank Prof. Rudi van Eldik (University of Erlangen-Nürnberg) for his support of this work. Markus Weitzer acknowledges the support from the DAAD (scholarship) and Prof. Andreas Zuberbühler (University of Basel, Switzerland) for allowing him to spend six very fruitful months in the research group of Prof. Zuberbühler.

References

1 M. Becker, S. Schindler and R. van Eldik, *Inorg. Chem.*, 1994, **33**, 5370.
2 S. Ryan, H. Adams, D. Fenton, M. Becker and S. Schindler, *Inorg. Chem.*, 1998, **37**, 2134.
3 S. Schindler, C. D. Hubbard and R. van Eldik, *Chem. Soc. Rev.*, 1998, **27**, 387.
4 M. Becker, F. Heinemann and S. Schindler, *Chem. Eur. J.*, 1999, **5**, 3124.
5 M. Becker, S. Schindler, K. D. Karlin, T. K. Kaden, S. Kaderli, T. Palanché and A. Zuberbühler, *Inorg. Chem.*, 1999, 1989.
6 M. Becker, F. Heinemann, F. Knoch, W. Donaubauer, G. Liehr, S. Schindler, G. Golub, H. Cohen and D. Meyerstein, *Eur. J. Inorg. Chem.*, 2000, 719.
7 S. Schindler, *Eur. J. Inorg. Chem.*, 2000, 2311.
8 M. Schatz, M. Becker, F. Thaler, F. Hampel, S. Schindler, R. R. Jacobsen, Z. Tyeklár, N. N. Murthy, P. Ghosh, Q. Chen, J. Zubieta and K. D. Karlin, *Inorg. Chem.*, 2001, **40**, 2312.
9 M. Schatz, M. Becker, O. Walter, G. Liehr and S. Schindler, *Inorg. Chim. Acta*, 2001, **324**, 173.
10 K. D. Karlin and A. D. Zuberbühler, in *Bioinorganic Catalysis*, 2nd edn., ed. J. Reedijk and E. Bouwman, Marcel Dekker, New York, 1999.
11 W. Kaim and J. Rall, *Angew. Chem.*, 1996, **108**, 47.
12 N. Kitajima, *Adv. Inorg. Chem.*, 1992, **39**, 1.
13 N. Kitajima and Y. Moro-oka, *Chem. Rev.*, 1994, **94**, 737.
14 *Bioinorganic Chemistry of Copper*, ed. K. D. Karlin and Z. Tyeklár, Chapman and Hall, New York, 1993.
15 E. Spodine and J. Manzur, *Coord. Chem. Rev.*, 1992, **119**, 171.
16 H.-C. Liang, M. Dahan and K. D. Karlin, *Curr. Opin. Chem. Biol.*, 1999, **3**, 168.
17 K. D. Karlin, *Science*, 1993, **261**, 701.
18 S. Fox and K. D. Karlin, in *Active Oxygen in Biochemistry*, ed. J. S. Valentine, C. S. Foote, A. Greenberg and J. F. Liebman, Blackie Academic and Professional, Chapman & Hall, Glasgow, 1995.
19 A. G. Blackman and W. B. Tolman, in *Structure and Bonding*, ed. B. Meunier, Springer, Berlin, 2000.
20 *Bioinorganic Catalysis*, 2nd edn., ed. J. Reedijk and E. Bouwman, Marcel Dekker, New York, 1999.
21 R. R. Jacobson, Z. Tyeklár, A. Farooq, K. D. Karlin, S. Liu and J. Zubieta, *J. Am. Chem. Soc.*, 1988, **110**, 3690.
22 Z. Tyeklár, R. Jacobson, R., N. Wei, N. Murthy, J. Zubieta and K. D. Karlin, *J. Am. Chem. Soc.*, 1993, **115**, 2677.
23 K. D. Karlin, N. Wei, B. Jung, S. Kaderli, P. Niklaus and A. D. Zuberbühler, *J. Am. Chem. Soc.*, 1993, **115**, 9506.
24 K. D. Karlin, S. Kaderli and A. D. Zuberbühler, *Acc. Chem. Res.*, 1997, **30**, 139.
25 E. Hörmann, M. Weitzer, B. Jung, S. Kaderli, A. D. Zuberbühler and S. Schindler, manuscript in preparation.
26 C. Geyer and S. Schindler, *Organometallics*, 1998, **17**, 4400.
27 A. L. Feig, M. Becker, S. Schindler, R. van Eldik and S. J. Lippard, *Inorg. Chem.*, 1996, **35**, 2590.
28 R. W. Cruse, S. Kaderli, K. D. Karlin and A. D. Zuberbühler, *J. Am. Chem. Soc.*, 1988, **110**, 6882.
29 R. W. Cruse, S. Kaderli, C. J. Meyer, A. D. Zuberbühler and K. D. Karlin, *J. Am. Chem. Soc.*, 1988, **110**, 5020.
30 J. A. Halfen, S. Mahapatra, E. C. Wilkinson, S. Kaderli, V. G. Young, L. Que, A. D. Zuberbühler and W. B. Tolman, *Science*, 1996, **271**, 1397.
31 D.-H. Lee, N. Wei, N. N. Murthy, Z. Tyeklar, K. D. Karlin, S. Kaderli, B. Jung and A. D. Zuberbühler, *J. Am. Chem. Soc.*, 1995, **117**, 12498.
32 H.-C. Liang, K. D. Karlin, R. Dyson, S. Kaderli, B. Jung and A. D. Zuberbühler, *Inorg. Chem.*, 2000, **39**, 5884.
33 S. Mahapatra, V. G. Young, S. Kaderli, A. D. Zuberbühler and W. B. Tolman, *Angew. Chem., Int. Ed. Engl.*, 1997, **36**, 130.
34 E. V. Rybak-Akimova, W. Otto, P. Deardorf, R. Roesner and D. H. Busch, *Inorg. Chem.*, 1997, **36**, 2746.
35 S. V. Kryatov, E. V. Rybak-Akimova, V. L. MacMurdo and L. Que, Jr., *Inorg. Chem.*, 2001, **40**, 2200.
36 B. S. Lim and R. H. Holm, *Inorg. Chem.*, 1998, **37**, 4898.
37 A. B. P. Lever, *Inorganic Electronic Spectroscopy*, 2nd edn., Elsevier, Amsterdam, 1984.
38 F. Thaler, C. D. Hubbard, F. W. Heinemann, R. van Eldik, S. Schindler, I. Fabian, A. M. Dittler-Klingemann, F. E. Hahn and C. Orvig, *Inorg. Chem.*, 1998, **37**, 4022.
39 H. Börzel, P. Comba, K. S. Hagen, H. Pritzkow, M. Schatz, S. Schindler and O. Walter, *Inorg. Chem.*, submitted for publication.
40 M. Kodera, K. Katayama, Y. Tachi, K. Kano, S. Hirota, S. Fujinami and M. Suzuki, *J. Am. Chem. Soc.*, 1999, **121**, 11006.
41 Z. Hu, R. D. Williams, D. Tran, T. G. Spiro and S. M. Gorun, *J. Am. Chem. Soc.*, 2000, **122**, 3556.
42 K. D. Karlin, D.-H. Lee, S. Kaderli and A. D. Zuberbühler, *Chem. Commun.*, 1997, 475.
43 E. F. Caldin, J. E. Crooks and A. Queen, *J. Phys. E: Sci. Instrum.*, 1973, **6**, 930.
44 K. D. Karlin, M. S. Nasir, B. I. Cohen, R. W. Cruse, S. Kaderli and A. D. Zuberbühler, *J. Am. Chem. Soc.*, 1994, **116**, 1324.
45 A commercial low temperature high pressure stopped-flow unit based on the design of Merbach and coworkers is commercially available from Hi-Tech Scientific.
46 M. Weitzer, M. Schatz and S. Schindler, work in progress.
47 J. H. Espenson, *Chemical Kinetics and Reaction Mechanisms*, McGraw-Hill, Inc., New York, 1995.
48 H. Gampp, M. Maeder, C. J. Meyer and A. D. Zuberbühler, *Talanta*, 1985, **32**, 95.

49 H. Gampp, M. Maeder, C. J. Meyer and A. D. Zuberbühler, *Talanta*, 1985, **32**, 257.

50 H. Gampp, M. Maeder, C. J. Meyer and A. D. Zuberbühler, *Talanta*, 1985, **32**, 1133.

51 H. Gampp, M. Maeder, C. J. Meyer and A. D. Zuberbühler, *Talanta*, 1986, **33**, 943.

52 M. Maeder and A. D. Zuberbühler, *Anal. Chem.*, 1990, **62**, 2220.

53 K. D. Karlin, S. Kaderli and A. D. Zuberbühler, *Acc. Chem. Res.*, 1997, **30**, 139.

54 J. Mandel, C. Maricondi and B. Douglas, *Inorg. Chem.*, 1988, **27**, 2990.

55 M. N. Burnett and C. K. Johnson, ORTEP3, Report ORNL-6895, Oak Ridge National Laboratory, Oak Ridge, TN, 1996.

56 SHELXTL, version 5.03, Siemens Analytical X-Ray Instruments, Madison, WI, 1997.